The IES Journal Part A: Civil & Structural Engineering
Publication details, including instructions for authors and subscription information:
http://www.informaworld.com/smpp/title~content=t781715625

Experimental investigation of edge restraint on punching shear behaviour of RC slabs

A.K.M. Jahangir Alam [a]; Khan Mahmud Amanat [a]; Salek M. Seraj [a]
[a] Department of Civil Engineering, Bangladesh University of Engineering and Technology, Dhaka, Bangladesh

Online Publication Date: 01 February 2009

To cite this Article Jahangir Alam, A.K.M., Amanat, Khan Mahmud and Seraj, Salek M.(2009)'Experimental investigation of edge restraint on punching shear behaviour of RC slabs',The IES Journal Part A: Civil & Structural Engineering,2:1,35 — 46

To link to this Article: DOI: 10.1080/19373260802449537

URL: http://dx.doi.org/10.1080/19373260802449537

The IES Journal Part A: Civil & Structural Engineering
Vol. 2, No. 1, February 2009, 35–46

Taylor & Francis
Taylor & Francis Group

TECHNICAL PAPER

Experimental investigation of edge restraint on punching shear behaviour of RC slabs

A.K.M. Jahangir Alam*, Khan Mahmud Amanat and Salek M. Seraj

Department of Civil Engineering, Bangladesh University of Engineering and Technology, Dhaka, Bangladesh

(*Received 1 June 2008; final version received 3 September 2008*)

Current codes of practice usually do not consider the effect of edge restraint on the punching shear capacity of flat plate type reinforced concrete structures. As the punching shear provisions incorporated in various codes of practice are a direct result of the empirical procedures, they do not usually provide an accurate estimation of the ultimate punching load capacity of a slab with its edges restrained against rotation. This is because no account is taken of the enhancement of punching capacity due to the in-plane restraint in many types of reinforced concrete slab systems. A total of 16 model slabs with restrained and unrestrained edges have been tested in an effort to ascertain the influence of boundary restraint, thickness of the slabs on their structural behaviour and punching load-carrying capacity. Edge restraint has been provided by means of edge beams of various dimensions in order to mimic the behaviour of continuous slabs. The cracking pattern and load-deflection behaviour of the slabs tested have also been monitored closely.

Keywords: edge restraint; column; concrete; punching shear; flat slab; membrane action

1. Introduction

Punching shear is an important consideration in the design of reinforced concrete flat plates, flat slabs and column footings. Present design rules for punching shear failure of reinforced concrete slabs, given in various codes of practice, are largely based on studies of the behaviour and strength of simply-supported, conventional specimens extending to the nominal line of contraflexure (Kuang and Morley 1992, Alam 1997). The code provisions rely mostly on empirical methods derived from the test results on conventional (Salim and Sebastian 2003) and thin slab specimens (Lovrovich and McLean 1990). In a continuous slab, all panel edges cannot rotate freely, in contrast to its simply supported counterpart. As a result, these codes may not properly mimic the punching shear behaviour of continuous and actual slab construction.

Test results from simply supported slab specimens do not usually provide an accurate prediction of the ultimate load capacity of a slab having lateral restraint. When the slab is restrained against lateral deformation, this induces large restraining force within the slab and between the supports, thus membrane forces are developed (Salim and Sebastian 2003). The enhancement of punching shear capacity can be attributed to the presence of in-plane compressive membrane action in the slab (Fenwick and Dickson 1989, McLean *et al.* 1990, Kuang and Morley 1992, Alam 1997, Salim and Sebastian 2003). The effect of compressive membrane stresses due to edge restraint has not been incorporated in the code formulations, resulting in conservative prediction of punching capacity.

In the presence of edge beams, the restraining effects of the slab on the rotation of beam also increase the strength of edge beam (Loo and Falamaki 1992). This reduces the moment of the column-slab interface, thus indirectly increasing the punching shear capacity. Slab deflection at column junction in the presence of edge beam also affects the punching shear capacity.

Some of the present-day code provisions usually specify the punching shear strength as a function of concrete strength alone. These codes do not adequately account for the possible role of specimen size and edge restraint. Under such circumstances, this study comprising a planned series of testing on restrained as well as unrestrained slabs is deemed essential in order to have an insight on the reasonable punching behaviour of reinforced concrete slabs.

2. Experimental procedure

A total of 16 square reinforced concrete slab specimens have been constructed and tested in this study. All of them had 1200 mm clear span except 16th specimen, which had a clear span of 1450 mm. Thirteen of these slabs had edge restraints in the form of edge beams, whereas the other three samples were plain normal slabs having no edge beam. The width of edge beam,

*Corresponding author. Email: alamj@buet.ac.bd

ISSN 1937-3260 print/ISSN 1937-3279 online

DOI: 10.1080/19373260802449537
http://www.informaworld.com

slab thickness and reinforcement ratio were the variable parameters for different samples. Details of the slab samples are given in Table 1 and typical plan and sectional details of slabs with edge beam are shown in Figure 1. Photographs of slab sample with reinforcement can be seen in Figures 2 and 3.

The experimental model slabs with edge restraints consist of a typically isolated slab-beam panel system where the slab panel was supported and restrained on all four sides by edge beams. The edge beams were integrally connected to the slab, and the strength ratio of the beam to slab was such that the beams remain elastic until failure of the slab. The different degrees of restraint imposed at the slab edges were provided by three different magnitudes of rigidity of the edge beams by varying the beam width (i.e. 245 mm, 175 mm and 105 mm). For the slabs without edge restraint (SLAB13, SLAB14 and SLAB15), slab thicknesses of 80 mm and 60 mm and reinforcement ratios ρ of 0.5% and 1.0% were provided. Although these slabs had supports on all four corners, an absence of integrally connected edge beams allowed the sides of the slabs to rotate during testing. In Table 2, the tested slab samples have been grouped on the basis of their edge restraint.

The samples SLAB1, SLAB2, SLAB3, SLAB7, SLAB10 and SLAB13 had 80 mm thickness with a span-to-depth ratio of 15. Samples SLAB4, SLAB5, SLAB6, SLAB8, SLAB9, SLAB11, SLAB12, SLAB14 and SLAB15 had 60 mm thick slab with a span-to-depth ratio of 20. SLAB16 had a clear span of 1450 mm and had a 60 mm thickness giving span-to-depth ratio of 24.17. Three reinforcement ratios, i.e. 0.5%, 1.0% and 1.5% in both directions were selected. The details are shown in Table 3.

3. Materials

The concrete used in the specimens consisted of ordinary Portland cement, natural sand and crushed stone aggregate with maximum size of 10 mm. The water–cement ratio for concrete was 0.45. Both 6 mm and 10 mm diameter plain steel bars having an average yield strength of 421 MPa were used in the slab panels and stirrups of edge beams. Flexural reinforcement in the edge beams were provided by 16 mm diameter deformed bars with average yield strength 414 MPa. An average cylinder compressive strength of 36 MPa at the age of 28 days was obtained from trial mixes.

4. Testing program

Each slab was subjected to concentrated loading at the geometric centre using a universal testing machine. Four steel blocks were used at each extreme corner of the slab as support and shown in Figure 4. During testing, corners of each sample were properly anchored. Loading was applied to specimen at an approximately constant rate up to the peak load. Deflections were measured at the same time. Failure occurred abruptly in all specimens and loading was terminated after failure.

Table 1. Details of reinforced concrete slab specimens.

Slab sample	Width of edge beam (b) mm	Slab thickness (h) mm	Reinforcement ratio (ρ) %	Main bars in each direction No.-mm ϕ	Extra top bars in each direction No.-mm ϕ	Edge beam reinforcement No.-mm ϕ
SLAB1	245	80	0.5	15-6	15-6	4-16
SLAB2	245	80	1.0	30-6	30-6	4-16
SLAB3	245	80	1.5	16-10	16-10	4-16
SLAB4	245	60	0.5	11-6	11-6	4-16
SLAB5	245	60	1.0	22-6	22-6	4-16
SLAB6	245	60	1.5	33-6	33-6	4-16
SLAB7	175	80	1.0	30-6	30-6	4-16
SLAB8	175	60	0.5	11-6	11-6	4-16
SLAB9	175	60	1.0	22-6	22-6	4-16
SLAB10	105	80	1.0	30-6	30-6	4-16
SLAB11	105	60	0.5	11-6	11-6	4-16
SLAB12	105	60	1.0	22-6	22-6	4-16
SLAB13	0	80	1.0	30-6	30-6	*3-16
SLAB14	0	60	0.5	11-6	11-6	*3-16
SLAB15	0	60	1.0	22-6	22-6	*3-16
SLAB16	340	60	1.0	26-6	26-6	4-16

*These reinforcements were provided at the extended bottom section of slab.
All stirrups for edge beam were 6 mm ϕ @ 88 mm c/c.
For SLAB1 to SLAB15, span = 1200 mm and for SLAB16, span = 1450 mm.
Clear cover of slab from bar centre = 10 mm.

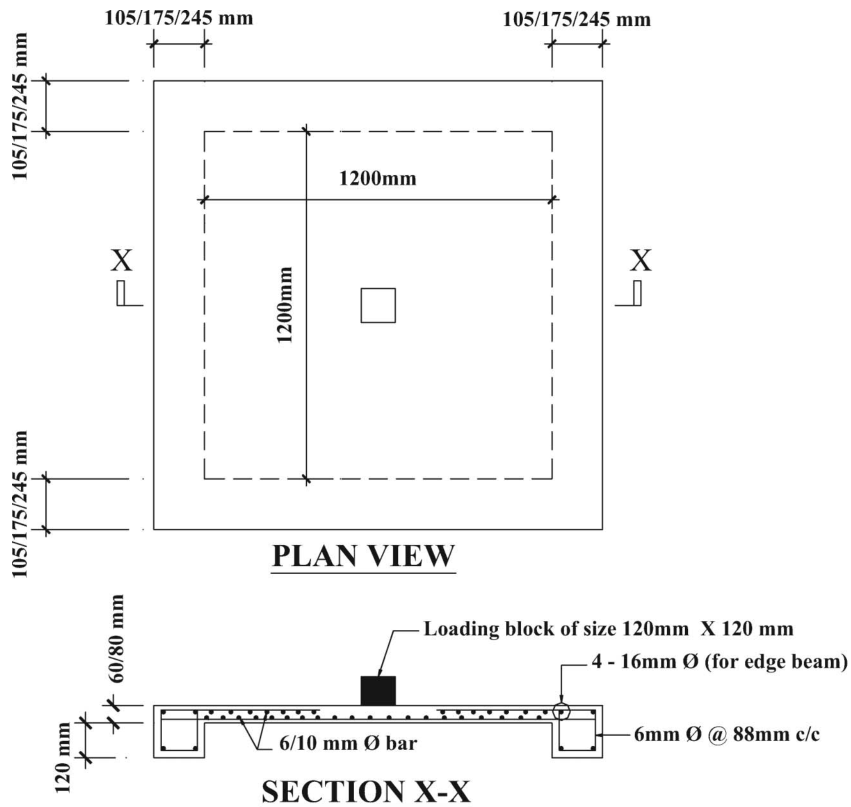

Figure 1. Details of a typical model slab with reinforcement.

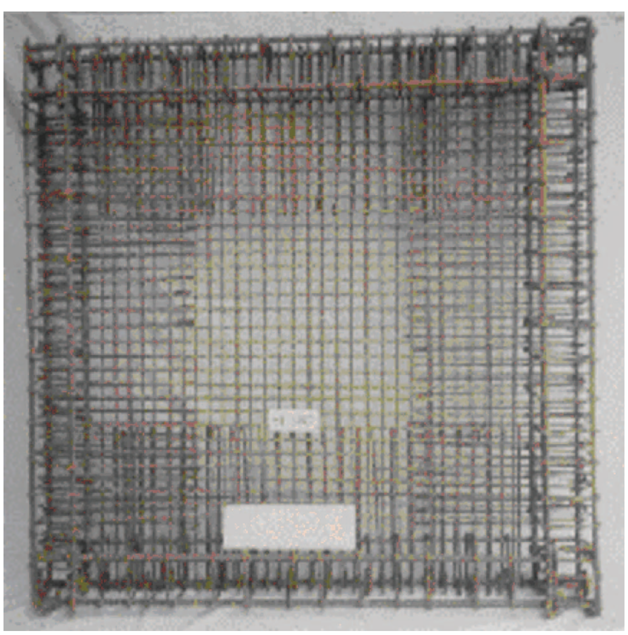

Figure 2. Photograph of typical model slab with reinforcement.

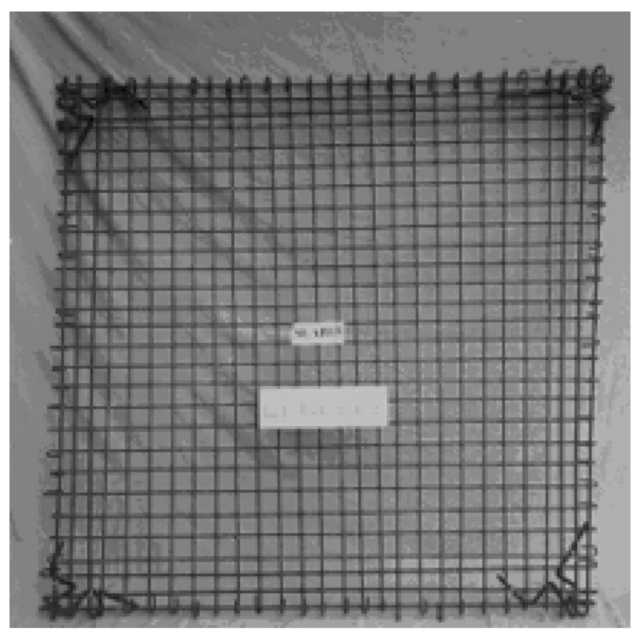

Figure 3. Photograph of typical model slab without edge beam.

A test rig (consisting mainly of steel girder, 300 kN capacity hydraulic jack) was used for the purpose of loading the slabs of various sizes under loading arrangements till failure. The load from the jack was applied to the model slabs at their geometric centres through a 20 mm thick steel plate of

120 mm × 120 mm size, simulating a concentrated load. The applied load was measured using an accurately calibrated load cell. Loading was applied to the specimens in increments of 8.90 kN up to 71.17 kN and then in increments of 4.45 kN up to failure with measurements of deflections after each increment of loading. The test set-up and testing arrangement are shown in Figures 4 and 5.

There was one LVDT at the mid-span to measure the central slab deflection. Another LVDT was placed at the middle span of one of the edge beams to measure the central vertical deflection of the edge beam and four LVDTs at the corner of edge beams to assess the performance of the supports.

Table 2. Slab grouping based on size of edge restraint.

Slab group	Width of edge beam (mm)	Slab sample
GROUP 1	245	SLAB1, SLAB2, SLAB3, SLAB4, SLAB5, SLAB6
GROUP 2	175	SLAB7, SLAB8 and SLAB9
GROUP 3	105	SLAB10, SLAB11 and SLAB12
GROUP 4	0	SLAB13, SLAB14 and SLAB15
GROUP 5	340	SLAB16

Table 3. Slab grouping based on reinforcement ratios.

Reinforcement ratio in percent	Slab sample
0.50	SLAB1, SLAB4, SLAB8, SLAB11 and SLAB14
1.00	SLAB2, SLAB5, SLAB7, SLAB9, SLAB10, SLAB12, SLAB13, SLAB15 and SLAB16
1.50	SLAB3 and SLAB6

5. Experimental results

All the models underwent punching type of failure with its inherent brittle characteristics. Most of the slab samples failed at a load much higher than those predicted by the codes. The cracking pattern of the top surface of all the slabs were very much localised and approximately had a size of average 120 mm × 120 mm as shown in Figure 6. The cracking patterns at the bottom surface of slabs having low percentage of reinforcement were more severe than those having higher percentages of steel. It was observed that the surface area of cracked zone for the slabs having wider edge beams were more than those slabs having smaller edge beams. It was also observed for all samples that the deflection at the support was negligible, indicating that the support fixity was ensured, albeit approximately, during the testing of the models. A typical crack pattern after failure on the bottom surface of slab model is shown in Figure 7.

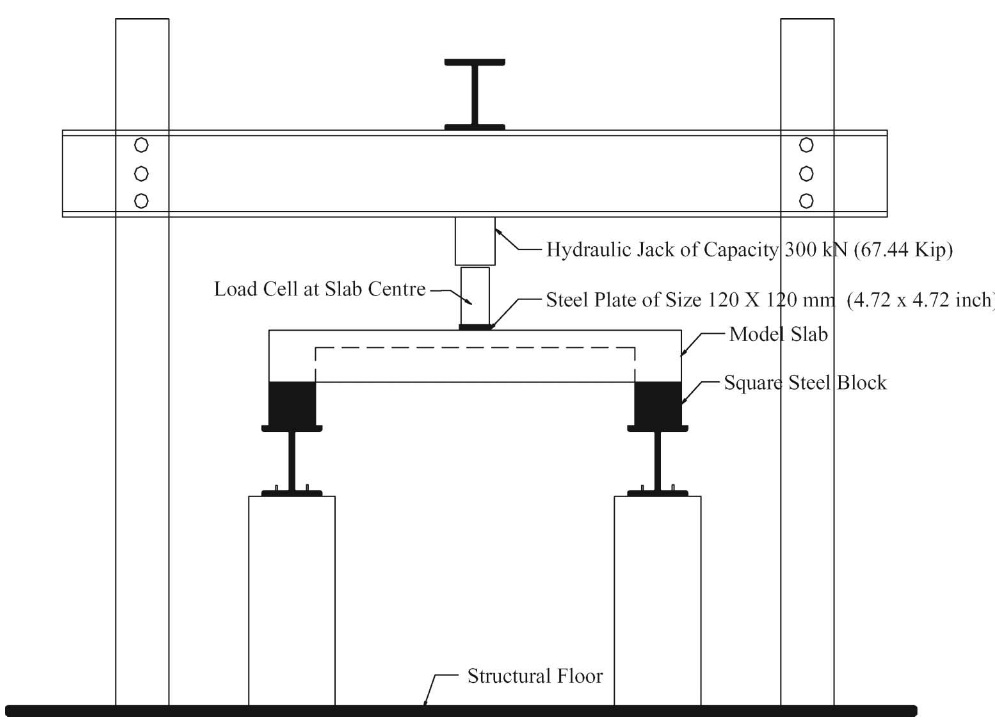

Figure 4. Testing set-up.

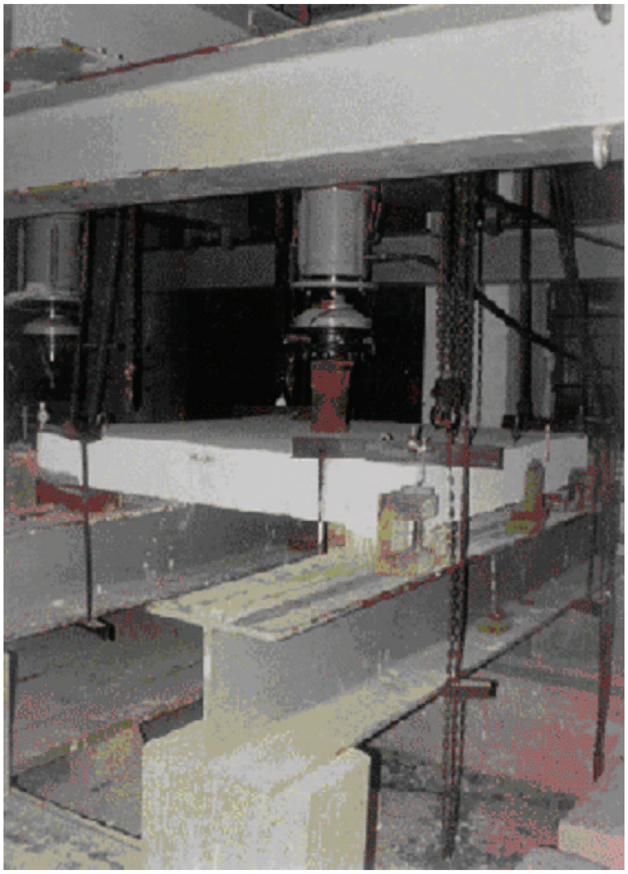

Figure 5. Test rig and testing arrangement.

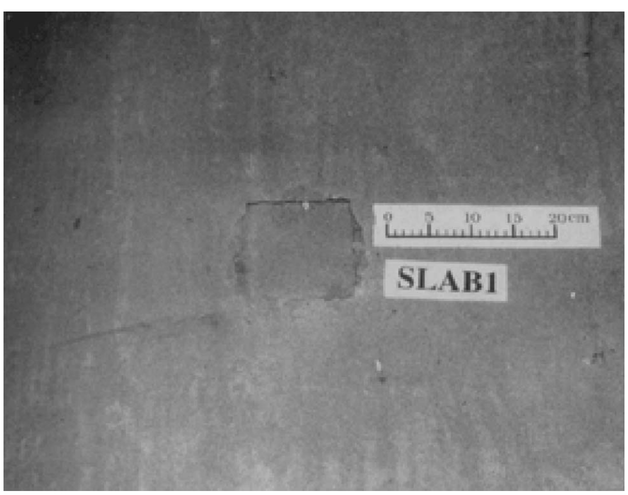

Figure 6. Typical cracking pattern on the top surface of a model slab.

6. Discussion of results

Test results obtained were analysed and shown in Tables 4 and 5. It has been found that ultimate punching shear capacity and behaviour of slab samples are dependent on the restraining action of slab edges, reinforcement ratio, slab thickness, and, of course, span-to-depth ratio of the slab. Apart from studying the ultimate punching load capacity, the effect of edge restraint and cracking patterns of the model slabs tested, detailed investigation has been carried out in order to find out the deficiency of current code provisions related to punching shear strength of slabs.

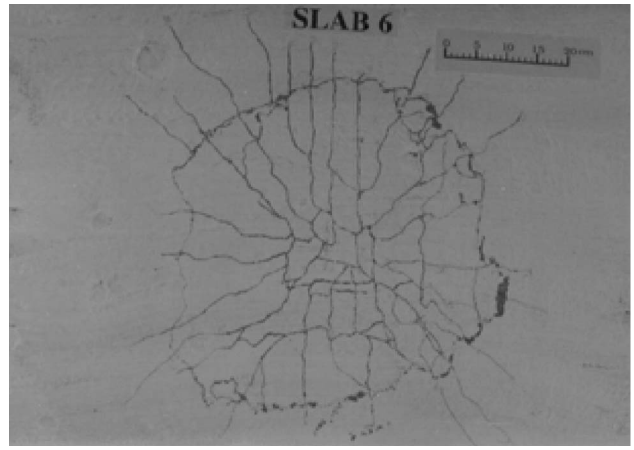

Figure 7. Typical cracking pattern on the bottom surface of a model slab.

6.1. *Deflection*

The variation of slab deflection with applied load of all slabs is shown in Figure 8. It may be recalled that complete load-deflection curves of the entire slab tested could not be traced due to the limitation of available instruments. It is, however, clear from Figures 9, 10 and 11 that central slab deflections were smaller for the slabs restrained by edge beams. The value of deflection decreased, in general, as the degree of edge restraint increased. In general, for smaller span to depth ratio of sample, the slab deflections at centre were smaller than those of higher span to depth ratio.

6.2. *Ultimate load carrying capacity*

All slab panels, failed in a punching shear mode. An analysis of test results is presented in Table 4, where non-dimensional punching shear strength [$P_u/f_c' b_0 d$, d = effective depth of slab, $b_0 = 4 \times (120 + d)$ mm, $b_0 = 4 \times (4.72 + d)$ inch] normalised punching shear strength ($P_u/\sqrt{fc'}\, b_0 d$) and normalised punching shear strength in accordance with the ACI code ($P_u/0.33\sqrt{fc'}\, b_0 d$, ignoring ϕ factor) of each specimen have been given. In this case, non-dimensional

Table 4. Non-dimensional and normalised punching shear strength of reinforced concrete slabs.

Slab sample	Width of edge beam mm	Experimental failure load (P_u) kN	Cylinder strength (f'_c) MPa	Non-dimensional strength	Normalised punching shear strength	Normalised punching shear strength using ACI formula
SLAB1	245	225.16	38.51	0.1099	0.6820	2.0667
SLAB2	245	242.09	37.42	0.1216	0.7439	2.2542
SLAB3	245	142.95	28.19	0.0953	0.5061	1.5336
SLAB4	245	138.12	38.24	0.1062	0.6569	1.9906
SLAB5	245	147.59	36.60	0.1186	0.7175	2.1742
SLAB6	245	130.51	41.95	0.0915	0.5927	1.7960
SLAB7	175	181.64	32.45	0.1052	0.5994	1.8164
SLAB8	175	133.27	41.30	0.0949	0.6099	1.8481
SLAB9	175	115.51	33.14	0.1025	0.5902	1.7885
SLAB10	105	188.89	37.45	0.0948	0.5802	1.7582
SLAB11	105	112.88	40.43	0.0821	0.5221	1.5821
SLAB12	105	115.73	37.04	0.0919	0.5593	1.6948
SLAB13	0	171.96	37.72	0.0857	0.5263	1.5948
SLAB14	0	84.73	34.71	0.0718	0.4230	1.2818
SLAB15	0	91.76	33.03	0.0817	0.4696	1.4230
SLAB16	340	171.96	40.24	0.1257	0.7973	2.4161

Table 5. Comparison of load carrying capacity with code predictions.

Slab models	Expt. failure load in kN	Predicted ultimate load in kN				Experimental failure load/code predicted load			
		ACI 318	BS 8110	CAN3-A23.3	CEB-FIP	Expt./ACI	Expt./BS	Expt./CAN	Expt./CEB
SLAB1	225.16	108.95	104.77	132.06	139.23	2.07	2.15	1.70	1.62
SLAB2	242.09	107.39	132.00	130.17	152.98	2.25	1.83	1.87	1.59
SLAB3	142.95	93.21	144.85	112.98	126.66	1.53	0.99	1.27	1.12
SLAB4	138.12	69.38	66.60	84.10	89.73	1.99	2.07	1.64	1.54
SLAB5	147.59	67.88	83.91	82.28	97.60	2.17	1.76	1.79	1.51
SLAB6	130.51	72.67	96.05	88.09	106.89	1.80	1.36	1.48	1.22
SLAB7	181.64	100.01	132.00	121.22	139.12	1.82	1.38	1.50	1.31
SLAB8	133.27	72.11	66.60	87.40	94.45	1.85	2.00	1.52	1.41
SLAB9	115.51	64.59	83.91	78.29	91.34	1.79	1.38	1.48	1.26
SLAB10	188.89	107.44	132.00	130.22	153.06	1.76	1.43	1.45	1.23
SLAB11	112.88	71.34	66.60	86.48	93.12	1.58	1.69	1.31	1.21
SLAB12	115.73	68.29	83.91	82.77	98.38	1.69	1.38	1.40	1.18
SLAB13	171.96	107.82	132.00	130.69	158.80	1.59	1.30	1.32	1.08
SLAB14	84.73	66.10	66.60	88.12	84.11	1.28	1.27	0.96	1.01
SLAB15	91.76	64.48	83.91	78.16	91.14	1.42	1.09	1.17	1.01
SLAB16	172.0	71.2	83.9	86.3	104.0	2.42	2.05	1.99	1.65
Average						1.81	1.57	1.49	1.31

punching shear strength has been calculated by dividing the corresponding ultimate load by the product of the compressive strength of concrete and critical surface at half the effective depth away from the perimeter of loaded area. The experimental punching shear strength has been normalised by dividing the corresponding load by the product of the square root of compressive strength of concrete and area of the nominal critical surface located at half the effective depth away from the perimeter of the load. Although SLAB6 had higher reinforcement, it failed at a lower test load than SLAB5. Excessive amount of reinforcement sometimes make structural concrete brittle as reported by Seraj *et al.* (1995).

Slab thickness and reinforcement ratio of SLAB16 were akin to those of SLAB5, SLAB9, SLAB12 and SLAB15. It is interesting to note from Table 4 that the degree of enhancement in the punching shear carrying capacity of SLAB16 was, in fact, slightly higher than the model slabs having smaller plan area. This reinforces the notion that the positive influence of edge restraint is not dependent on slab size and that the general trend shown by model slabs are also reflected in slabs having larger dimensions. However, since only one slab having

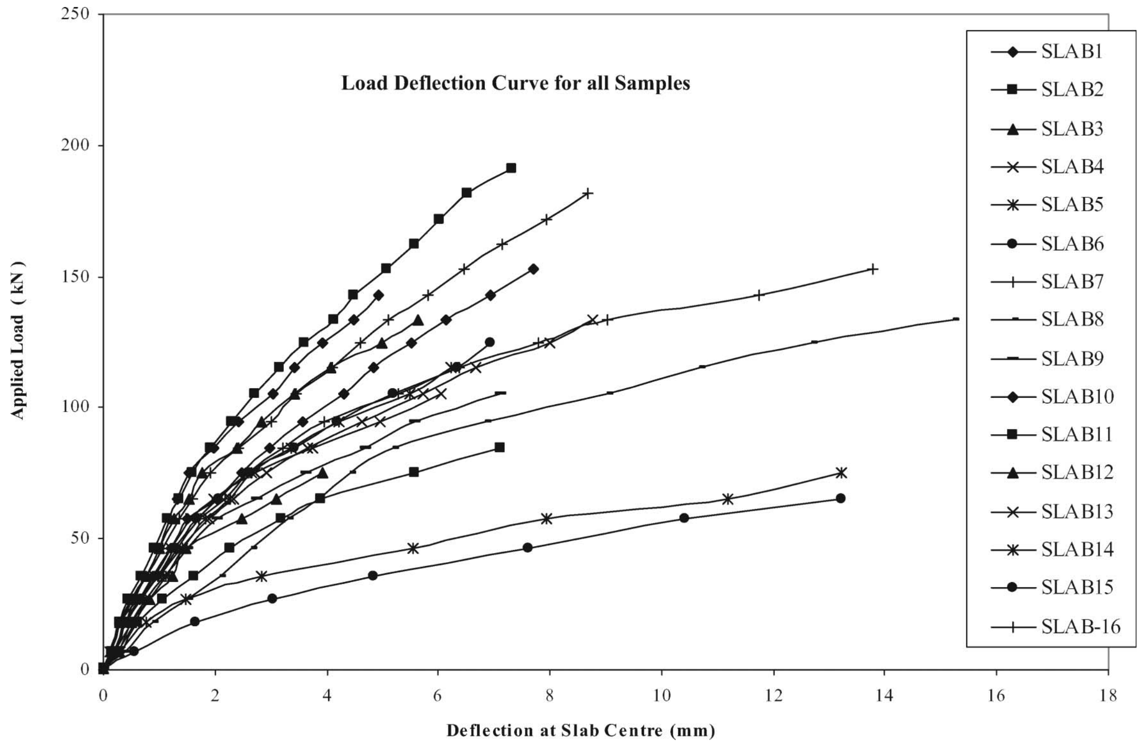

Figure 8. Deflection at slab centre of all slabs under different loading.

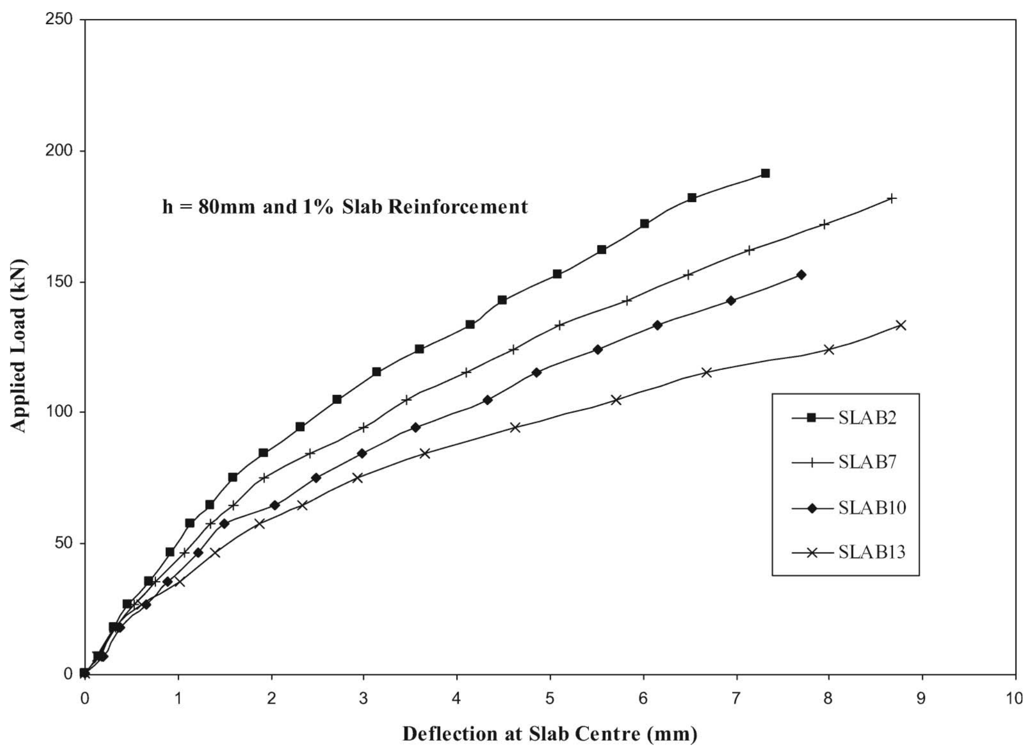

Figure 9. Deflection at centre of slab with $h = 80$ mm and 1% slab reinforcement under different loads.

slightly larger dimension was tested in this study, further tests are, of course, needed to understand the possible influence of size effect on punching load capacity. The findings of the present study, thus, may be considered to be applicable, albeit tentatively, to all sorts of slabs.

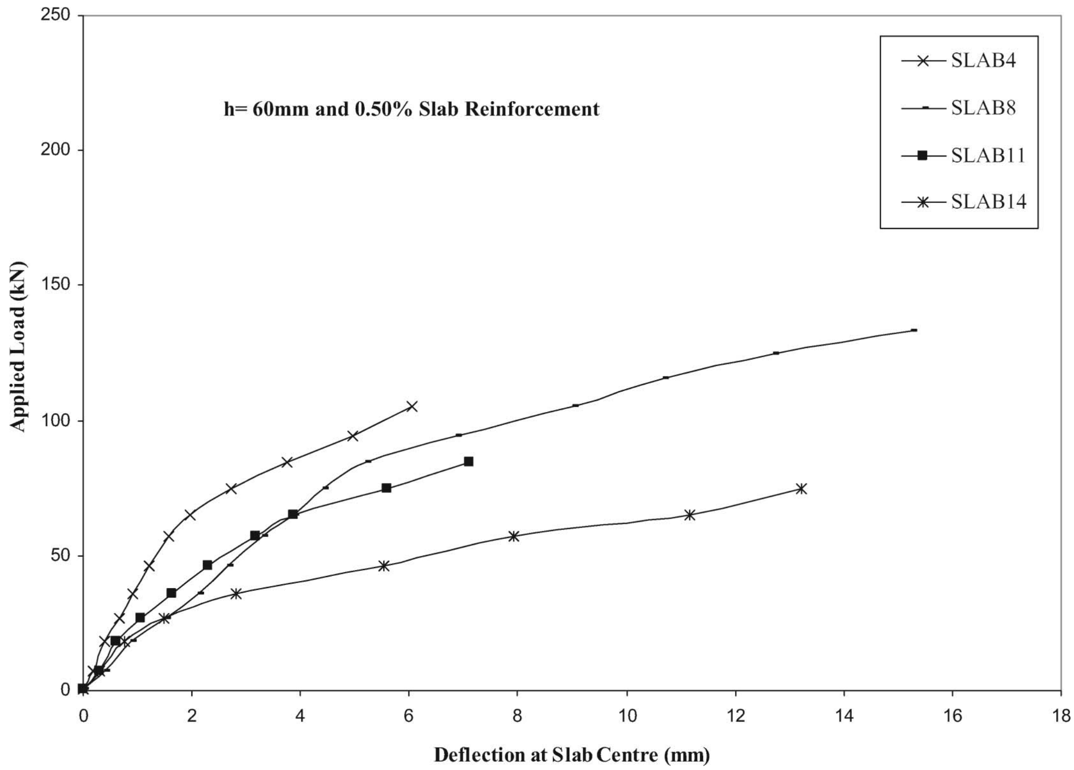

Figure 10. Deflection at centre of slab with $h = 60$ mm and 0.50% slab reinforcement under different loads.

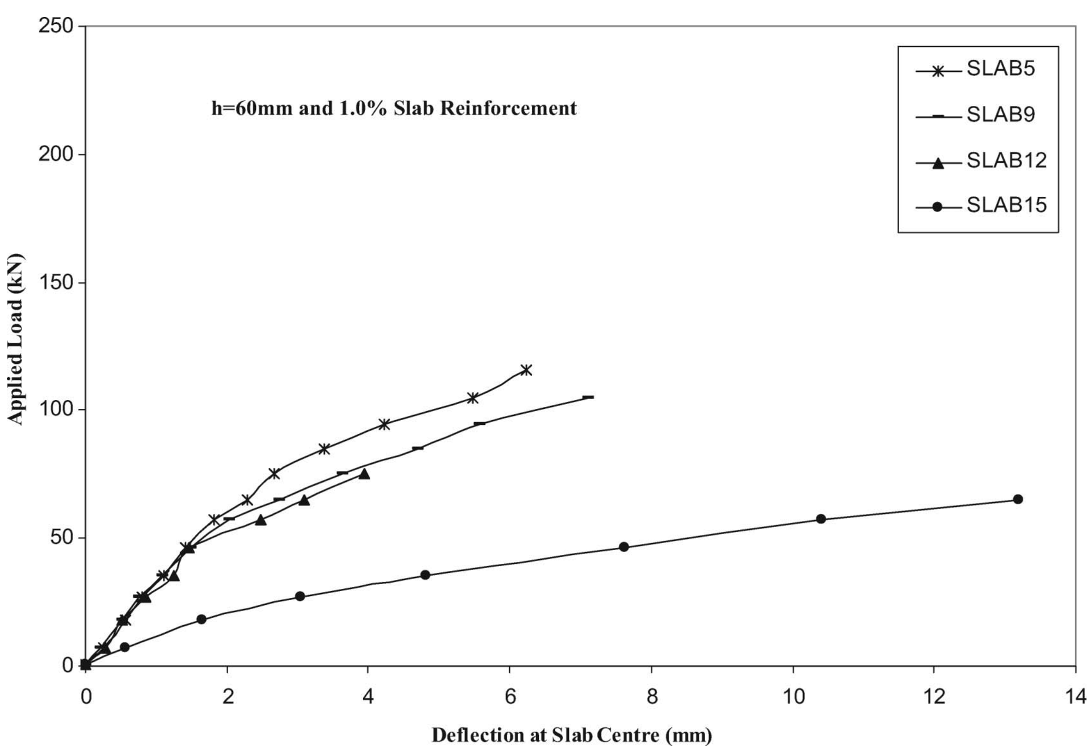

Figure 11. Deflection at centre of slab with $h = 60$ mm and 1% slab reinforcement under different loads.

6.3. *Effect of edge restraint*

Table 4 shows that there was a definite increase in punching load of the slab panels as the degree of edge restraint increased. This trend is also evident in Figure 12, where punching shear capacity increased significantly with the increase in the width of edge beams up to 245 mm. Reinforcement ratio and slab thickness have been taken to be constant for each curve in Figure 12.

The present exercise reveals that the edge restraint has a significant effect on the ultimate punching load of reinforced concrete slabs, resulting in a significant increase of punching shear resistance in the slabs and effectively enhancing the load-carrying capacity of the member subjected to punching load. The enhancement in the punching load carrying capacity of slabs due to edge continuity may be attributed to the possible influence of in-plane restraint. This may be due to the lateral slab expansion and possible restraint against outward movement by the edge beams. Continuous slabs deflect less than similar simply supported slabs under the action of load. This helps the slabs having edge continuity to sustain more punching load (Alam 1997).

Enhancement of punching shear capacity due to restraint action was also advocated by other researchers like Salim and Sebastian (2003), Kuang and Morley (1992), Lovrovich and McLean (1990), McLean *et al.* (1990) and Rankin and Long (1987). Similar to the findings of other researchers, compressive membrane forces were, in fact, developed in the slabs due to edge restraints.

The enhancement of load carrying capacity can also be attributed to the presence of in-plane compressive membrane action in the slab (Fenwick and Dickson 1989). Membrane action generally occurs after cracking of the concrete or yielding of the reinforcement, and has been found to result in substantial enhancement in the load carrying capacity of restrained concrete slabs (Kuang and Morley 1992). These arise from the coupling of in-plane and bending deformations in flexurally cracked reinforced concrete members and the restraint in the in-plane deformation provided by the surrounding structure and the boundaries (Fenwick and Dickson 1989).

The restraining effects of the slab produce a higher load carrying capacity for the spandrel beam in flat plate slab when compared with an isolated beam. This increase in capacity is a result of the slab restraints on both the elongation and the rotation of the edge beam (Loo and Falamaki 1992). Apart from this, the rotation of spandrel beam also produces a vertical displacement at the beam slab interface. The vertical displacement will be restrained by the vertical stiffness of slab. The restraining effects of the slab on the rotation of beam also increase the strength of beam (Loo and Falamaki 1992), thereby reducing the moment of the column-slab junction and indirectly increasing the punching shear capacity.

In a normal simply supported reinforced concrete design, the neutral axis is located closer to the compression face of the member, and so strain of the middle depth of the slab is tensile over the full length, indicating expansion. Conventionally, this length

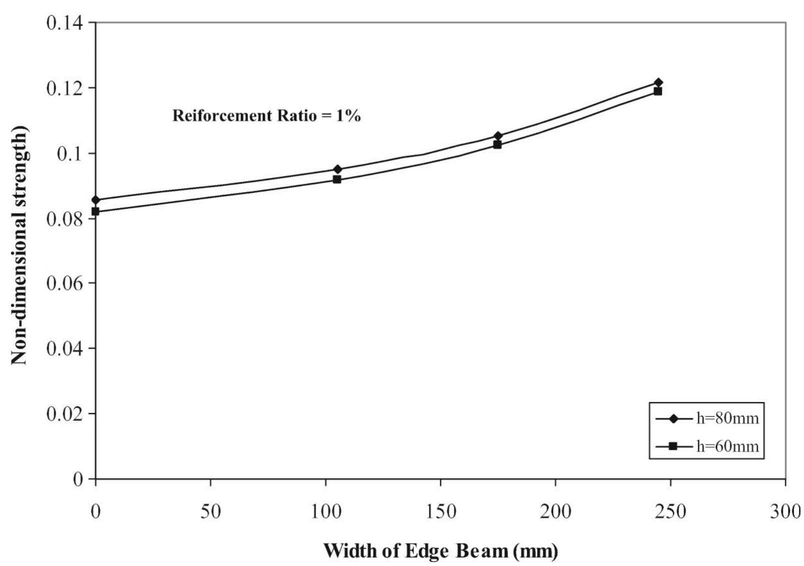

Figure 12. Effect of edge restraint for 1.0% reinforcement.

change is ignored. In practice, this expansion results in a compressive force that enhances the performance of the member by reducing the magnitude of the tensile force required in the reinforcement for a given load (Fenwick and Dickson 1989). Thus, slab deflection at column junction in the presence of edge beam also affects the punching shear capacity.

6.4. *Cracking*

During tests, the development of cracking and the width of cracks were carefully observed and monitored at various load increments. Cracking on the underside of the slabs developed as a series of cracks radiating from the centrally loaded area. As the load increases, the widths of the cracks also increase as expected.

Cracking pattern at the bottom surface of models having same slab thickness and reinforcement (as shown in Figures 13–16), were fine and cracks were large in number in case of strongly restrained slabs. For moderately restrained slabs, such cracks were found to be wider and fewer in number. In case of strongly restrained slabs, due to the presence of in-plane forces, the width of the cracks was less and consequently the total energy due to punching was distributed among a large number of fine cracks (Kuang and Morley 1992, Alam 1997). On the other hand, in slabs having lesser amount of lateral restraint, initially produced cracks could widen and thereby, the total energy was distributed to lesser but wider cracks. The discontinuity on the top surface of the slabs after punching typically took the square geometry of the punching plate size of average 120 mm × 120 mm.

The crack widths of the normally reinforced ($\rho = 1.0\%$) and heavily reinforced ($\rho = 1.5\%$) slabs were found to be smaller than those of lightly reinforced slabs ($\rho = 0.5\%$). Whilst cracks of slabs with reinforcement level of 0.5% propagated more readily towards the edges, similar cracks for other slabs having more reinforcement were somewhat concentrated in the middle portion of the slab.

7. Comparison of test results with different code predictions

The load-carrying capacities of all slab models obtained from tests as well as from the predictions of ACI 318-05 (2005), BS 8110-97 (1997), CAN3-A23.3-M04 (2004) and CEB-FIP (1990) are summarised in Table 5. All terms related to various factors of safety have been made equal to 1.0. While calculating the predicted strength of slabs, the actual compressive (cylinder) strength of concrete on the day of testing was used. Where necessary, compressive cube strength

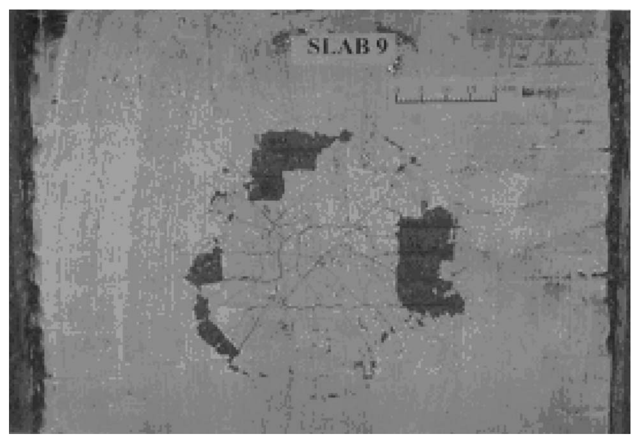

Figure 14. Cracking of bottom surface for $h = 60$ mm, $\rho = 1\%$ and $b = 175$ mm (SLAB9).

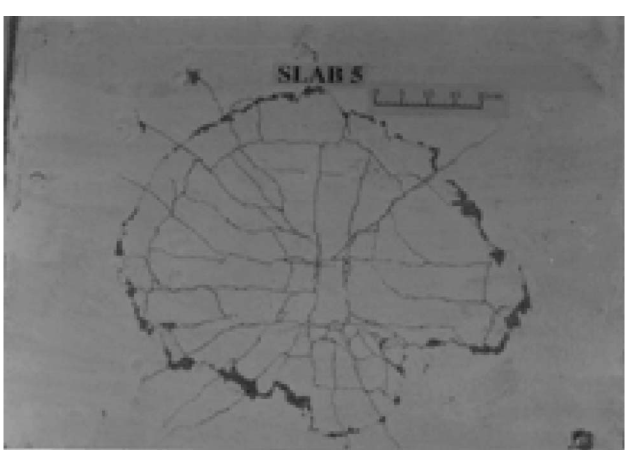

Figure 13. Cracking of bottom surface for $h = 60$ mm, $\rho = 1\%$ and $b = 245$ mm (SLAB5).

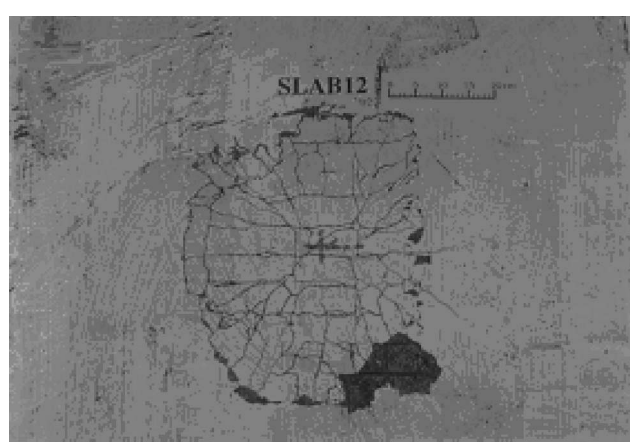

Figure 15. Cracking of bottom surface for $h = 60$ mm, $\rho = 1\%$ and $b = 105$ mm (SLAB12).

has been estimated to be 25% higher than its cylinder strength counterpart. A bar graph is also presented in Figure 17. This figure represents experimental and ultimate predicted load capacities calculated by various code of practices.

It is evident in Table 5 and Figure 17, for both 80 mm and 60 mm thick slabs, that the experimental load carrying capacity is much higher than those predicted by the codes. American code (ACI 318-05) has been found to be more conservative than the other codes while the European code (CEB-FIP-1990) was the closest to the experimental values. The British code (BS 8110-97) and the Canadian code (CAN3-23.3-M04) predictions fell in between the American and European codes.

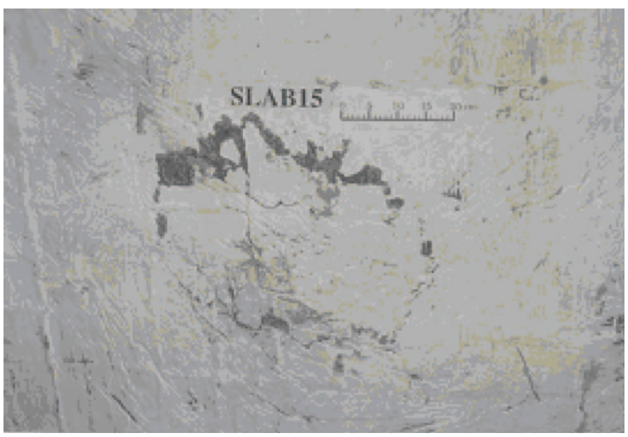

Figure 16. Cracking of bottom surface for $h = 60$ mm, $\rho = 1\%$ and no edge beam (SLAB15).

SLAB16 was a 60 mm thick slab with 1.0% reinforcement ($\rho = 1.0\%$). The width of the edge beam of this slab ($b = 340$ mm) was higher than all other slab samples of this study. The clear span of this slab was also greater than all other slab samples and was equals to 1450 mm. The area of this slab was, thus, 46% higher than all other slabs investigated in this study. From Table 5, it can be seen that the load carrying capacity of this slab was greater than those predicted by ACI 318-05, BS 8110-97, CAN3-A23.3-M04 and CEB-FIP-1990 by 2.42, 2.05, 1.99 and 1.65 times, respectively.

It appears that, for slab samples having 0.5% reinforcement, load carrying capacities predicted by the European and Canadian codes were closer to the experimental load carrying capacities for slabs having zero restraint. In this case, for restrained slabs, European code was, once again, found to be less conservative than all other codes. The American and British codes were most conservative in predicting the capacity of slabs having $\rho = 0.5\%$. They also predicted similar conservative punching capacity.

It is also evident that the experimental load carrying capacity of the slabs increases with increasing degree of edge restraint provided by edge beams of larger widths. This restraining action of slabs has not been taken into consideration in any of the code provisions.

In view of the fact that ACI 318-05 is, perhaps, the most widely used code in the world and also it seems to form the basis of Bangladesh National Building Code BNBC (Bangladesh National Building Code 1993), the normalised punching shear strength using ACI code

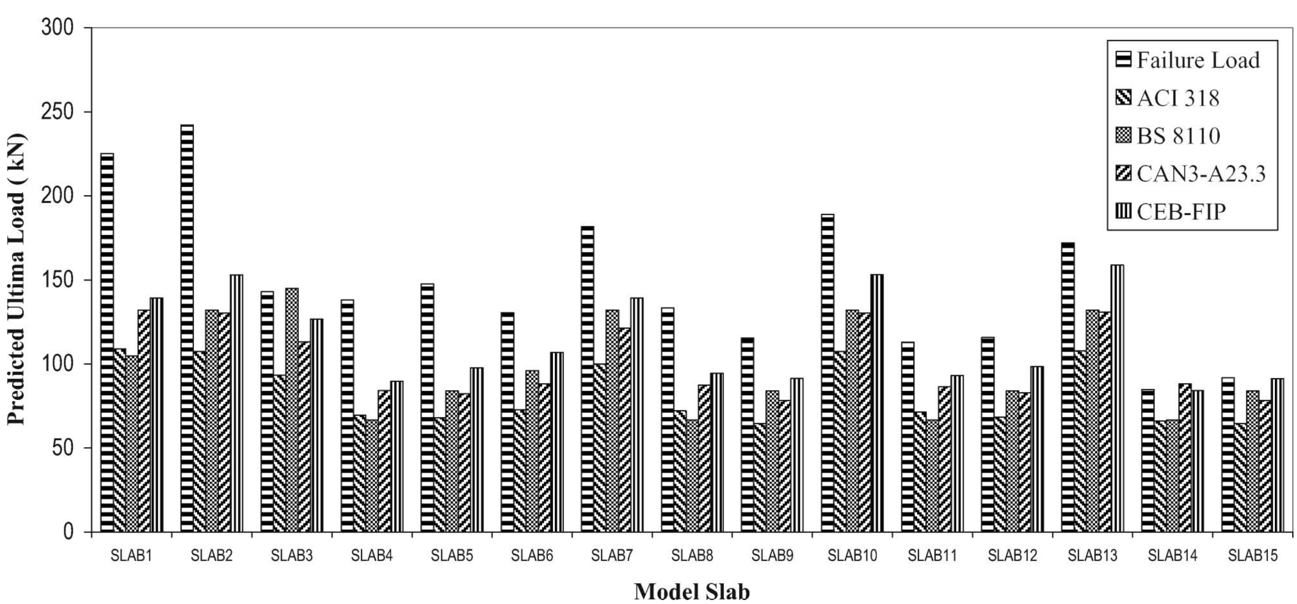

Figure 17. Experimental failure load and predicted ultimate load in accordance with different codes.

formula ($P_u/0.33\sqrt{f_c'}\,b_0d$) for different edge restraints as well as reinforcement ratios are only 0.33 times $\sqrt{f_c'}\,b_0d$. In reality, it may attain much higher values. Further testing may lead to possible modifications in code provisions due to the dangerous nature of shear failure. CAN3-A23.3-M04 already uses slightly higher values of 0.4 in a similar equation.

From the foregoing discussion, it can be concluded that the present codes may not be capable of predicting the punching shear strength of reinforced concrete slabs satisfactorily taking into account the effect of edge restraint. For all the slabs tested, the prediction of ACI 318-05 was most conservative. On the other hand, although European code (CEB-FIP code) predictions were very much on the conservative side, its prediction of punching failure load was better and more economical than the others. In general, all the codes failed to some degree to cater for the beneficial effect of edge restraint.

8. Conclusions

Punching tests on sixteen reinforced concrete slabs have been reported herein. Thirteen of these slabs are restrained at the edges to simulate continuous slab construction. The tests results provided some basic experimental information on the behaviour of restrained slabs subjected to concentrated loading. All the slabs failed in a punching mode when subjected to punching load at the slab centre. The outcome of the present series of tests may become useful for the development of a rational method of analysis. Whereas the following conclusions may be derived from the limited experimental work reported herein, further experimental research on a wide range of slabs is, of course, needed to consolidate the findings.

(a) Punching shear strengths observed from punching tests conducted on the restrained reinforced concrete slabs have been found to be higher than the predictions of present-day code provisions. Present code methods underestimate the punching load capacity of slabs as the code provisions are based on tests conducted on simply supported slabs with their edges unrestrained. The magnitude of the strength enhancement increases with the degree of edge restraint.

(b) The degree of enhancement in the punching shear capacity due to continuity at the slab edges (imposed by edge beams) do not diminish with increasing size of slabs.

References

ACI Committee 318, 2005. *Building code requirements for reinforced concrete (ACI 318–05)*. Detroit: American Concrete Institute.

Alam, A.K.M.J., 1997. *Punching shear behavior of reinforcement concrete slabs*. M.Sc. Engineering Thesis, Department of Civil Engineering, Bangladesh University of Engineering & Technology.

Bangladesh National Building Code, 1993. Prepared for Housing and Building Research Institute. Dhaka, Bangladesh.

BS 8110, 1997. *Structural use of concrete: part 1: code of practice for design and construction*. London: British Standard Institution.

CAN3-A23.3-M04, 2004. *Design of concrete for buildings*. Rexdale: Canadian Standards Association.

CEB-FIP, 1990. Model code for concrete structures. *Comite Euro-International du Beton*. London: Cement and Concrete Association.

Fenwick, R.C. and Dickson, A.R., 1989. Slabs subjected to concentrated loading. *ACI Structural Journal (American Concrete Institute)*, 86 (6), 672–678.

Kuang, J.S. and Morley, C.T., 1992. Punching shear behavior of restrained reinforced concrete slabs. *ACI Structural Journal*, 89 (1), 13–19.

Loo, Y.C. and Falamaki, M., 1992. Punching shear strength analysis of reinforced concrete flat plates with spandrel beams. *ACI Structural Journal*, 89 (4), 375–383.

Lovrovich, J.S. and McLean, D.I., 1990. Punching shear behavior of slabs with varying span-depth ratios. *ACI Structural Journal*, 87 (5), 507–511.

McLean, D.I., Phan, L.T., Lew, H.S., and White, R.N., 1990. Punching shear behavior of lightweight concrete slabs and shells. *ACI Structural Journal*, 87 (4), 386–392.

Rankin, G.I.B. and Long, A.E., 1987. Predicting the enhanced punching strength of interior slab-column connections. *Proceedings of the Institution of Civil Engineers* (London), Part 1, 82, 1165–1186.

Salim, W. and Sebastian, W.M., 2003. Punching shear failure in reinforced concrete slabs with compressive membrane action. *ACI Structural Journal*, 100 (4), 471–479.

Seraj, S.M., Kotsovos, M.D., and Pavlovic, M.N., 1995. Behavior of high-strength mix reinforced concrete beams. *Journal of Archives of Civil Engineers, Proceedings Polish Academy of Sciences*, 41 (1), 31–67.